Electron emission in collisions between dressed Al^{q+} ions with He targets

J M Monti[1], J Fiol[2], D Fregenal[2], P D Fainstein[2], R D Rivarola[1], W Wolff[3], E Horsdal[4], G Bernardi[2], S Suárez[2]

[1] Laboratorio de Colisiones Atómicas. Instituto de Física Rosario (CONICET-UNR) and Facultad de Ciencias Exactas, Ingeniería y Agrimensura, Universidad Nacional de Rosario, Avenida Pellegrini 250, 2000 Rosario, Argentina

[2] Centro Atómico Bariloche, Comisión Nacional de Energía Atómica, 8400 San Carlos de Bariloche (Río Negro) and Consejo Nacional de Investigaciones Científicas y Técnicas (CONICET), Argentina

[3] Instituto de Física, Universidade Federal do Rio de Janeiro, PO 68528, 21941-972 Rio de Janeiro, RJ, Brazil

[4] Department of Physics and Astronomy, Aarhus University, DK-8000 Aarhus C, Denmark

E-mail: monti@ifir-conicet.gov.ar

Abstract. Experimental and theoretical results are presented for electron emission in collisions between dressed Al^{q+} ions and atomic He targets. The experimental data are compared with a four-body CTMC model and two distorted wave models, namely the CDW and CDW-EIS. The contribution to total electron emission spectra from the ionisation of each collision center and as well as the simultaneous ionisation can be assessed separately.

1. Introduction

The understanding of the dynamics of single- and multiple-electron emission is of great interest in many applications such as fusion reactors, space weather, radiation damage and hadrontheraphy. Thus, electron emission in collisions between dressed-ions and atomic and molecular targets has been a matter of increasing interest in the last few years. Nevertheless, the bibliography regarding experimental electron emission cross sections is still scarce.

In many-body collision systems, ionisation may take place as due to different identifiable physical mechanisms. At high impact energies, the role of the interaction of target's electrons with projectile's electrons may be separated from the role of the electron-nucleus interactions, and has been interpreted in terms of *screening* and *antiscreening* interactions [1]. In this context, antiscreening is associated with the collision of a quasi-free electron accompanying one center with the bound electron in the other. For intermediate impact energies, the binding energy cannot be neglected anymore and the clear separation between antiscreening and screening disappears. On the other hand, as the interaction time increases, the shell structure of the interaction potential may become important to the electron emission.

In this work we present experimental and theoretical results on electron emission in collision between swift dressed Al^{q+} ions ($q = 1, 2, 3$) and He targets. One interesting feature of these collision systems is that the binding energy of the projectile electrons is similar to the binding energy of the target electrons, thus projectile electrons can no longer be considered as

passive (frozen in their orbitals during all the reaction). Therefore, target, projectile and even simultaneous ionisation can give a noticeable contribution to electron emission.

Experimental doubly differential cross sections for electron emission induced by intermediate energy projectiles are compared to a four-body classical Classical Trajectory Monte Carlo (CTMC), in which electrons from both centres are considered. The interactions of the electrons with both nuclei as well as the interaction between electrons from different centres are shown to produce ionisation. Also two three-body quantum distorted wave theories, namely the Continuum distorted Wave (CDW) and the Continuum distorted Wave-Eikonal Initial State (CDW-EIS), have been used to calculate the differential cross sections. The extension of the CDW and CDW-EIS models to the case of dressed projectiles have been performed by Monti *et al.* in [2, 3]. The above mentioned CTMC and distorted wave models were recently applied to calculate electron emission cross-sections in collisions between Li^{q+} ($q = 1, 2$) and He [4].

2. Experimental setup and procedure

Energy distributions for total electron emission (TE) in collisions of Al^{q+} ($q = 1, 2, 3$) with He were measured for projectile incident energies ranging from 100 keV/u to 211 keV/u. The Al^{q+} beam was generated with the 1.7 MV Tandem accelerator at Centro Atómico Bariloche. Most of the experimental setup, including the acceleration, the beam transport section and the collision chamber, has been described in detail elsewhere [5, 6]. Briefly, a collimated projectile beam intersected an effusive gas target at the focus of a cylindrical mirror analyzer within the collision chamber. This spectrometer rotates in a plane perpendicular to the target flow direction so that electron distributions can be measured for any energy and angle on that plane [5]. After the collision, the projectiles were collected in a Faraday cup, and used to normalize the spectra. The background pressure in the collision chamber was below 5.3×10^{-7} mbar, while the pressure in the transport region, after the selector magnet, was lower than 4×10^{-6} mbar. During the experiment, when target gas was present, the pressure in the collision chamber rose to 4×10^{-5} mbar. For all measurements in this work, the angular acceptance was set to 2 degrees and the energy resolution of the electron analyzer was 6%.

All spectra were taken under the same experimental conditions, and several tests were performed to check data reproducibility. Spurious contributions due to collisions with the background gas in the chamber and in the transport sections were estimated and corrected from the data [5]. A reference distribution was measured for normalization purposes, ensuring the correct relative contribution of the different emission angles within an estimated uncertainty of 15%. Statistical errors are significant only for high-energy electron emission and for electrons emitted in the backward direction. Doubly differential cross-sections (DDCS) for electron emission at several energies and angles were determined from the experimental data [5]. In particular, DDCS were obtained for 105 keV/u Al^{+}, 106 keV/u and 156 keV/u Al^{2+}, and 211 keV/u Al^{3+} in collision with He targets.

3. Theory

3.1. CTMC

We have performed four-body Classical-Trajectory Monte-Carlo (CTMC) simulations of the Al^{q+} + He ionisation collisions. The measured spectra for the system under study, obtained by electron-spectroscopy, is the result of the combined contributions from target-ionisation, projectile-ionisation, and simultaneous ionisation from both centers. From a theoretical point of view, the description of these processes is complex because the dynamics of the collision is dictated by the combined action of the $(n^2 - n)/2$ pairs of interactions between the n particles involved. In the CTMC calculations performed in this work we have considered only one active electron on each center, while the action of the rest of the projectile electrons and the remaining electron in the target was incorporated in the atomic model potentials. This is equivalent to

consider a system with the following Hamiltonian:

$$\mathcal{H} = (\mathcal{H}_T + \mathcal{H}_P) + V_{N_P,N_T} + V_{N_P,e_T} + V_{N_T,e_P} + V_{e_T,e_P} \,, \tag{1}$$

where $\mathcal{H}_T$, $\mathcal{H}_P$ are the isolated-target and isolated-projectile Hamiltonians, that cannot produce the ionisation. The labels in the interaction terms correspond to target and projectile nucleus (N_T, N_P) and electrons (e_T, e_P), respectively. In the present work V_{N_P,N_T}, V_{N_P,e_T}, and V_{N_T,e_P} include the screening due to the passive electrons in each center, while the antiscreening contribution is explicitly included in the electron-electron interaction term. We have represented the interactions by means of two-parameters Green-Sellin-Zachor (GSZ) model potentials [7] (see next section).

The description of the collision system including electrons on both centers allows us to investigate the ionisation of both target and projectile, and shed some light on the role of the nucleus-electron and electron-electron interactions on the observed spectra.

3.2. Distorted wave models
Besides the CTMC calculations, we have computed electron emission by means of extensions of the CDW and CDW-EIS models for dressed projectiles, following the philosophy of previously introduced works on target ionisation [2, 3]. In the CDW model [8] the initial channel distorted wavefunction is written as the product of an initial target bound function, and a Coulomb continuum factor that describes the interaction between the target active electron and the projectile in the entry channel. After the ionisation, the electron evolves in the combined fields of the projectile and the residual target. The final channel distorted wavefunction is chosen as a target continuum state multiplied by a Coulomb continuum factor. In the CDW-EIS model the initial channel Coulomb continuum factor is replaced by its asymptotic form, given by an Eikonal phase [9].

To extend these models to the case of dressed projectiles [2, 3] the projectile potential V_{N_P,e_T} was represented by means of GSZ potentials [7, 10]. These potentials can be written as the sum of a short-range and a long-range terms, the latter due to the asymptotic screened projectile charge q:

$$V_{N_P,e_T}(s) \;=\; V^{lr}(s) + V^{sr}(s) \tag{2}$$

$$\;=\; -\frac{q}{s} - \frac{Z_P - q}{s}\left[H(e^{s/d} - 1) + 1 \right]^{-1} \tag{3}$$

with Z_P the projectile nuclear charge, s the distance of the target active electron to the projectile nucleus, and H and d parameters depending on Z_P and q (see [10]). With this choice for the projectile potential, the transition amplitude as a function of the impact parameter $\vec{\rho}$ results:

$$\mathcal{A}_{if}(\vec{\rho}) = \mathcal{A}_{if}^{sr}(\vec{\rho}) + \mathcal{A}_{if}^{lr}(\vec{\rho}) \tag{4}$$

where $\mathcal{A}_{if}^{lr}$ is the well known transition amplitude in the CDW or CDW-EIS models for a bare ion of charge q [8, 9], and $\mathcal{A}_{if}^{sr}$ is a term related to the short-range term of the potential V_{N_P,e_T}. The calculations of these terms within the distorted-wave models have been described in detail elsewhere [3].

For the case of projectile ionisation, the DDCS as a function of electron energy and emission angle are evaluated in the moving projectile reference-frame, and then transformed to the laboratory rest frame by means of the well known expression

$$\mathrm{DDCS}(\theta, \varepsilon) = \left(\frac{\varepsilon}{\varepsilon'} \right)^{1/2} DDCS(\theta', \varepsilon') \,, \tag{5}$$

where the primed (unprimed) quantities are associated with the projectile (laboratory) rest frame (see for example reference [4]).

In order to estimate the order of magnitude of the contributions of simultaneous ionisation from the target and the projectile (dielectronic ionisation) a probabilistic approach was used. If we consider the collision of a projectile Al^{q+} with a He target, the DDCS for simultaneous ionisation was calculated as

$$DDCS^{(sim)} = \frac{DDCS^{(P)}TCS^{(T)}}{TCS^{(P)} + TCS^{(T)}} + \frac{DDCS^{(T)}TCS^{(P)}}{TCS^{(P)} + TCS^{(T)}}, \tag{6}$$

where $DDCS^{(P)}$ corresponds to Al^{q+} projectile ionisation due to the interaction with a He target, $DDCS^{(T)}$ the He target ionisation by Al^{q+} impact, and $TCS^{(P,T)}$ are their corresponding total cross sections. This approach gives a very rough estimation of the simultaneous ionisation contribution, and does not take into account any interference effects. It is expected to be more suitable when electrons in one center are much deeper bound than in the other center, and has been previously employed for helium ionisation by lithium ions [4].

4. Results and Conclusions

In figures 1 and 2 experimental and theoretical DDCS for electron emission in collisions between 100 keVu^{-1}Al$^+$ and He atoms are presented as a function of the electron energy for a fixed emission angle of $0°$ and $10°$, respectively. In all figures the experimental results were normalized to the CDW values in order to match the profiles in the high energy region.
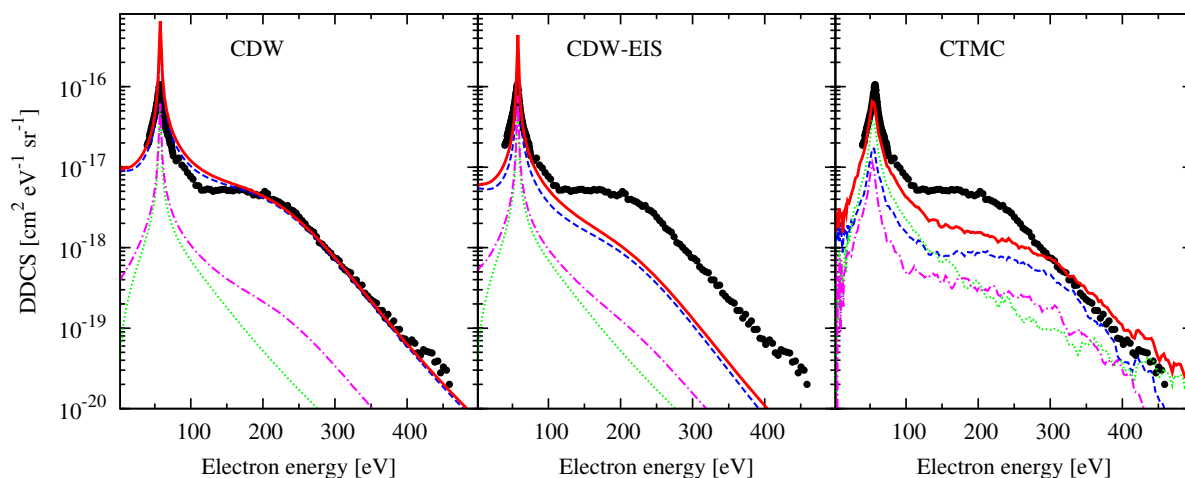
Figure 1. DDCS for electron emission in 105 keV/u Al$^+$ + He collisions as a function of the electron energy for a $0°$ fixed emission angle. Target ionisation $(- - -)$, projectile ionisation $(\cdots\cdots)$, simultaneous ionisation $(— \cdot —)$, TE $(——)$, and experimental results $(\bullet)$ are shown.

Two features stand out on the forward spectra: one of them, the cusp peak observed at electron velocities close to the projectile initial velocity, results from the contribution of the well-known target-electron capture to the continuum (ECC) and projectile-electron loss (ELP) cusps. The second is the broad shoulder observed above 200 eV that corresponds to strong quasi-binary collisions of the projectile with the target electron.

For $0°$ the CDW model gives a very good representation of the experiments while CDW-EIS does not represent appropriately the experimental results for emission energies above 100 eV. For $10°$, the CDW results overestimate the experiments for energies below 170 eV. Both quantum
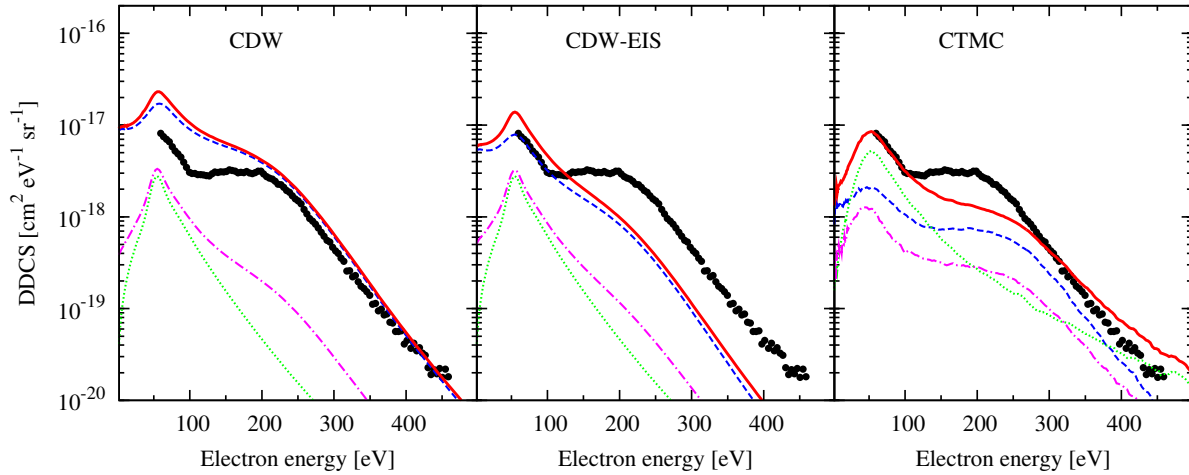
Figure 2. Same as Fig. 1 but for a $10°$ fixed emission angle.

theories predict that ECC mechanism is more important than ELP. On the other hand, CTMC agrees with the data at high and low electron energies but underestimates the experimental data in the binary-encounter energy region. In this case ELC appears more important than ECC.

Due to the relatively large number of electrons in the aluminium ions, the short-range part of the projectile-electron interaction plays a major role in the helium ionisation. This is probably the greater source of error in the CDW-EIS model, since the eikonal initial-state wavefunction does not behave correctly in the neighborhood of the origin of coordinates, where the short-range potential is relevant. Additionally, both distorted-wave models are perturbative theories, and are expected to perform better at large incident energies.

In figures 3 and 4 experimental and theoretical DDCS for electron emission at $0°$ are shown for 150 keVu^{-1} Al^{2+} + He, and 200 keVu^{-1} Al^{3+} + He, respectively. In both cases the CDW calculations give a good representation of the experimental data, whereas the CDW-EIS results largely underestimate them.

Figure 3 shows that the main contribution to the total electron emission (TE) comes from target ionisation, while projectile and simultaneous ionisation are only appreciable in the ECC cusp region. However, these latter contributions decrease dramatically for increasing values of the projectile charge q because the involved electrons are more strongly bound.

Since for Al^{3+} the only appreciable contribution is target ionisation, projectile and simultaneous ionisation contributions are not shown in figure 4 but were included in the total emission spectrum. Instead, the figure show the target electron emission due to the short- and long-range parts of the V_{N_P,e_T} potential. As expected from the complexity of the projectile, the short-range interaction is the main responsible for the observed cross sections at high emission energies. Thus, even when both models represent the contributions from the long-range part in a similar fashion, the contribution from the short-range part is, as discussed above, largely underestimated in the CDW-EIS model.

In conclusion, new experimental data and theoretical results were presented for electron emission in Al^{q+} + He ($q = 1, 2, 3$). No theory was able to describe satisfactorily the data for all emission angles and energies. Possible reasons for the discrepancies are the large number of electrons involved and the impact energy being too low for the perturbative quantum-mechanical approaches. Improvements to the model potentials and to the probabilistic treatment of simultaneous ionisation are currently in progress.
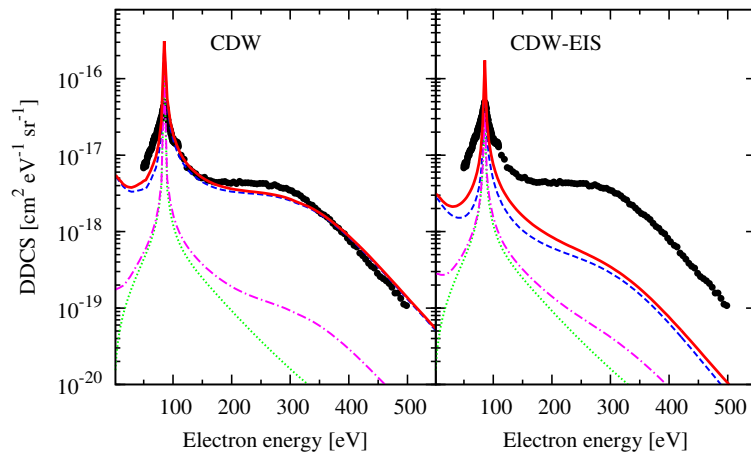
Figure 3. DDCS for electron emission in 156 keV/u Al^{2+}+He collisions as a function of the electron energy for a $0°$ fixed emission angle. Target ionisation ($- - -$), projectile ionisation ($\cdots\cdots$), simultaneous ionisation ($— \cdot —$), TE (——), and experimental results ($\bullet$) are shown.
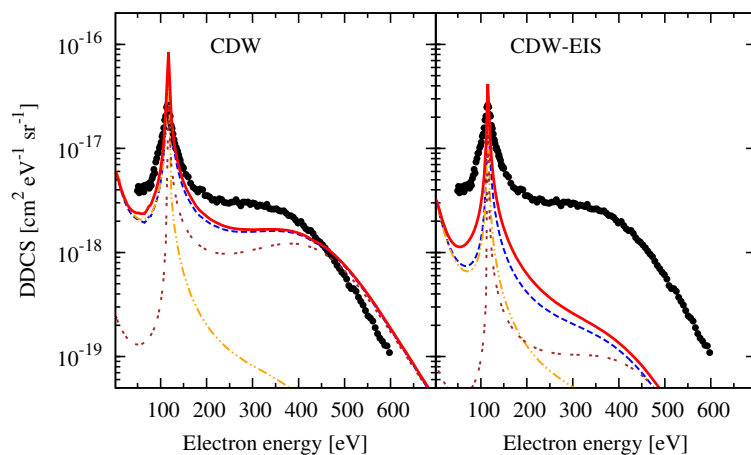
Figure 4. DDCS for 211 keV/u Al^{3+}+He ionisation collisions. Total electron emission (——), target ionisation ($- - -$), and contributions to target ionisation from the long-range ($— \cdot —$) and short-range (-- --) parts of the interaction are indicated.

References

[1] J. H. McGuire, N. Stolterfoht, and P. R. Simony. *Phys. Rev. A*, 24:97–102, 1981.
[2] J. M. Monti, R. D. Rivarola, and P. D. Fainstein. *J. Phys. B: At. Mol. Opt. Phys.*, 41:201001, 2008.
[3] J. M. Monti, R. D. Rivarola, and P. D. Fainstein. *J. Phys. B: At. Mol. Opt. Phys.*, 44:195206, 2011.
[4] J M Monti, J Fiol, D Fregenal, P D Fainstein, R D Rivarola, W Wolff, E Horsdal, G Bernardi, and S Suárez. *Phys. Scr.*, T156:14031, 2013.
[5] G. Bernardi, S. Suárez, D. Fregenal, P. Focke, and W. Meckbach. *Rev. Sci. Instrum.*, 67:1761–1768, 1996.
[6] J M Monti, D Fregenal, S Suárez, P D Fainstein, R D Rivarola, G Bernardi, and J Fiol. *J. Phys. B: At. Mol. Opt. Phys.*, 45:145202, 2012.
[7] A. E. S. Green, D. L. Sellin, and A. S. Zachor. *Phys. Rev.*, 1:184, 1969.
[8] Dž Belkić. *J. Phys. B: At. Mol. Opt. Phys.*, 11:3529, 1978.
[9] D. S. F. Crothers and J. F. McCann. *J. Phys. B: At. Mol. Opt. Phys.*, 16:3229–42, 1983.
[10] P. P. Szydlik and A. E. S. Green. *Phys. Rev. A*, 9:1885, 1974.